FACTA UNIVERSITATIS
Series: **Mechanical Engineering** Vol.1, N° 7, 2000, pp. 925 - 934

LOCAL STRESS AND STRAIN STATE IN THE REGION OF CRACK FOR DIFFERENT GLOBAL STRESS STATES IN A PLATE

UDC 539.4.014+539.37:539.421:624.073.1(045)

Dragan B. Jovanović[1], Milena B. Jovanović[2]

[1]Faculty of Mechanical Engineering, University of Niš
Beogradska 14, 18000 Niš, Yugoslavia, e-mail: jdragan@masfak.masfak.ni.ac.yu
[2]Vojvode Tankosića 9, 18000 Niš, Yugoslavia
e-mail: mjovanovic@masfak.masfak.ni.ac.yu

Abstract. *In a plate with different ruling cases of global or general stress state, different local stress, and strain states will appear at vicinity of the crack, as a result of interaction between crack geometry and global stress state. By taking in consideration of elliptically shaped crack (Griffith's crack), which can degenerate to slit, by giving one semi-axis equal to zero, and by introducing different general stress states, corresponding local stress and dislocation distributions at the vicinity of such crack were obtained. Previously was assumed that global stress state is plane and three-dimensional stress and displacement state at the vicinity of crack was obtained. Finite element method and three-dimensional model of the plate with crack was applied. Global loads were given in this way that stress in region of the plate without disturbances caused by crack are unit values, and normalization of local stresses related to global stresses was done.*

The conventional plate theories assume that the stress variations in terms of the thickness coordinate are known as a priori. For plane stress state, the transversal normal stress component σ_z *is assumed to be zero throughout the plate, and in-plane stresses* σ_x, σ_y, *and* τ_{xy} *are independent of thickness coordinate. These assumptions are valid under vary limited circumstances, and in the very narrow framework.*

Cases of global stress state, when axial tension forces are acting in direction perpendicular to the crack plane, or in direction of the crack, are considered. Graphical presentations of stress distribution of σ_x, σ_y, σ_z, τ_{xy}, τ_{yz}, τ_{zx}, *as well as displacements* u_x, u_y *and* u_z *are given in this paper.*

Evidently varying of stress tensor components is related to the coordinate **z** *perpendicular to the middle plane of the plate, and* σ_z *is different from zero up to certain distance from the crack tip. Based on obtained diagrams of stress distribution, and displacements distribution, conclusions about influence of global stress state on local distribution of stresses and displacements at surrounding of the crack were drawn out.*

Received August 01, 2000
Presented at 5th YUSNM Niš 2000, Nonlinear Sciences at the Threshold of the Third Millenium, October 2-5, 2000, Faculty of Mechanical Engineering University of Niš

1. INTRODUCTION. FRAMEWORK.

This paper is analyzing plate with Griffith's elliptical crack [1], [2], [11], [14], [15], and it is assumed that material is ideal elastic [16], with material constants for polyester Palatal P-6. Young's elasticity modulus is $E = 4460$ N/mm^2, and Poisson's modulus is $\nu = 0.38$ for Palatal P-6. It is assumed that global stress state is plane (two-dimensional) and it is given by uniform distributed loading forces $\sigma = 1$ N/mm^2 on the edge sides of the plate. Finite element method is used for determining of the stress tensor components and displacement components [10]. Three loading cases are taken in consideration in this paper:

- plate loaded by uniform distributed tension forces in **x** direction, as it is presented on Fig. 1,
- plate loaded by uniform distributed tension forces in **y** direction, as it is presented on Fig. 10,
- plate loaded by uniform distributed tension forces in **x**, and **y** direction, as it is presented on Fig. 19.

It is visible that third case is superposition of first and second loading case.

2. LOCAL STRESS AND STRAIN STATE FOR DIFFERENT GLOBAL STRESS STATES

Plate loaded in **x** direction is shown on Fig. 1. Distributions of stress components σ_x, σ_y, σ_z, τ_{xy} and τ_{zx} on the plate surface, and for section $y = 0$ are presented on Fig. 2, 3, 4, 5 and 6 respectively. It is visible that at the most part of plate, plane stress state is approved. Also, it is visible on Fig. 4 that stress component σ_z is different than zero at region close to crack tip, and that stress components σ_x and σ_y are nonlinearly distributed across the thickness in **z** direction, in the region close to crack tip.

Loads in this case are causing closure of the crack. Figures 7, 8, and 9 are presenting displacements u_x, u_y, and u_z. It is visible that crack didn't make influence on displacements in the plate.

Plate loaded in **y** direction is shown on Fig. 10. Distributions of stress components σ_x, σ_y, σ_z, τ_{xy} and τ_{zx} on the plate surface, and for section $y = 0$ are presented on Fig. 11, 12, 13, 14 and 15 respectively. It is visible that at the most part of plate plane stress state is approved. Also, it is visible on Fig. 13 that stress component σ_z is different than zero at region close to crack tip, and that stress components σ_x and σ_y are nonlinearly distributed across the thickness in **z** direction, in the region close to crack tip.

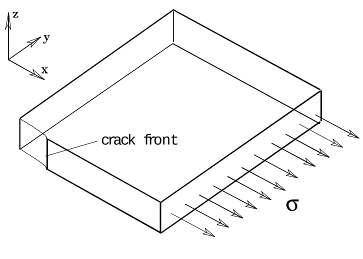

Fig. 1.

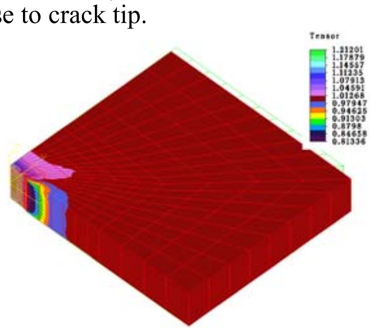

σ_X

Fig. 2.

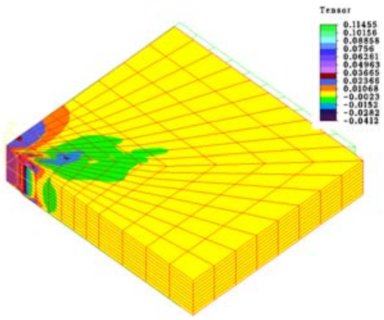

σ_Y

Fig. 3.

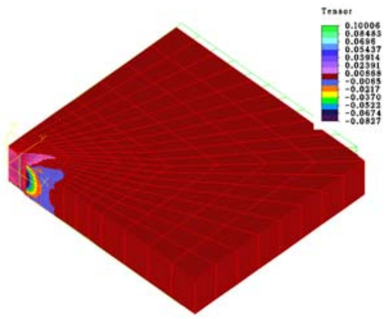

σ_Z

Fig. 4.

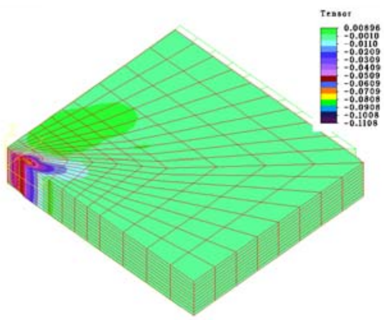

τ_{xy}

Fig. 5.

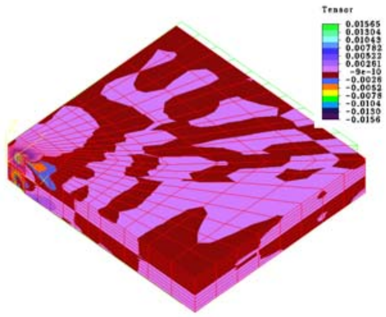

τ_{zx}

Fig. 6.

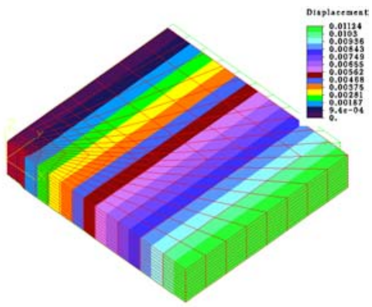

u_x

Fig. 7.

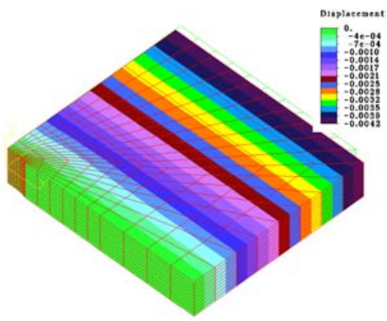

u_y

Fig. 8.

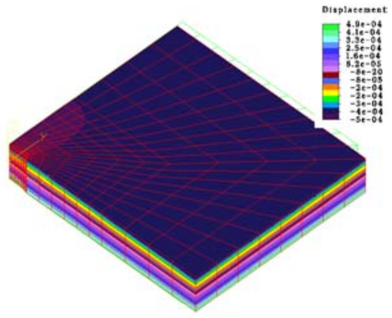

u_z

Fig. 9.

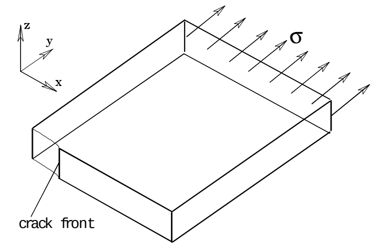

Fig. 10.

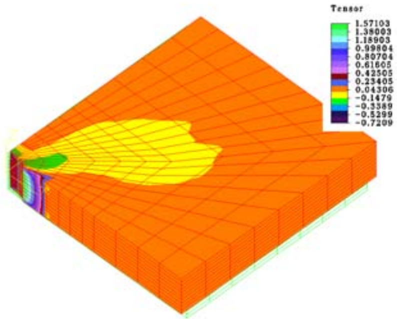

σ_x

Fig. 11.

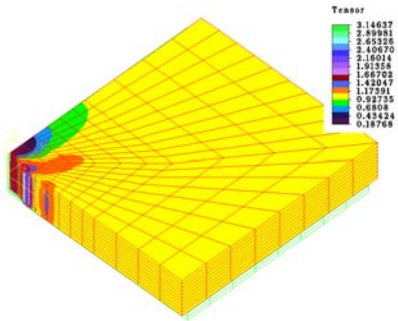

σ_y

Fig. 12.

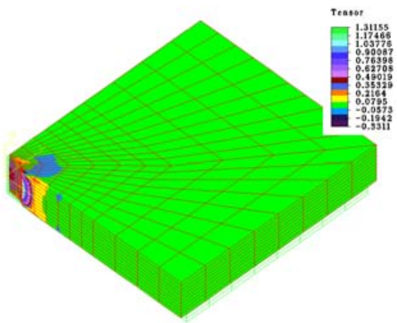

σ_z

Fig. 13

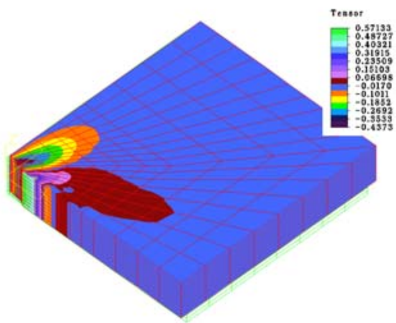

τ_{xy}

Fig. 14.

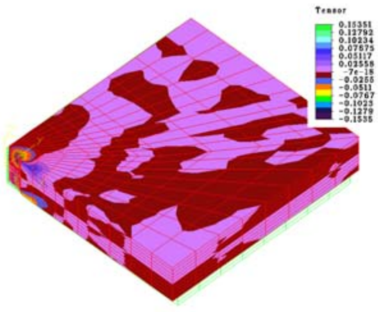

τ_{zx}

Fig. 15.

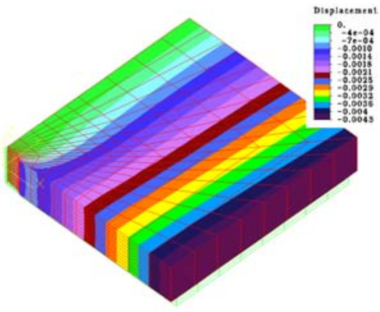

u_x

Fig. 16.

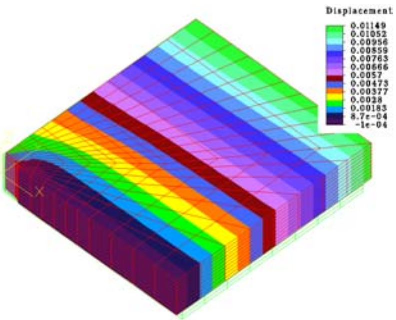

u_y

Fig. 17.

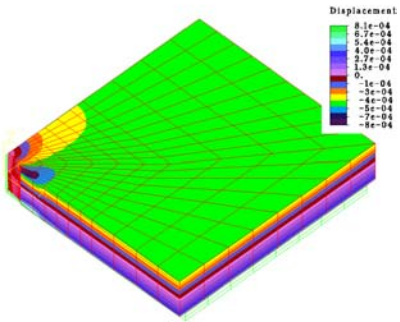

u_z

Fig. 18

Loads in this case are causing opening of the crack. It is visible on Fig. 16, 17, and 18, which are presenting displacements u_x, u_y, and u_z, that crack influenced on displacements in the plate. Contraction in **z** direction is higher on the crack tip then in the rest of the plate, and it is lower on the middle of crack contour than in the rest of the plate. It seems like contour line on the crack tip goes down, and middle of the crack contour x = 0 goes up.

Plate loaded in **x** and **y** direction is shown on Fig. 19. Distributions of stress components σ_x, σ_y, σ_z, τ_{xy} and τ_{zx} on the plate surface, and for section y = 0 are presented on Fig. 20, 21, 22, 23 and 24 respectively. It is visible that at the most part of plate plane stress state is ruling stress state. Also, it is visible on Fig. 22 that stress component σ_z is different than zero at region close to crack tip, and that stress components σ_x and σ_y are nonlinearly distributed across the thickness in **z** direction, in the crack tip vicinity.

Loads in **x** direction are causing closure, and loads in **y** direction are causing opening of the crack contour. It is visible on Fig. 25, 26, and 27, which are presenting displacements u_x, u_y, and u_z, that crack influenced on displacements in the plate, in same way like when loads in y direction are acting alone. Consequently, contraction in **z** direction is higher on the crack tip then in the rest of the plate, and it is lower on the middle of crack contour than in the rest of the plate. It seems like contour line on the crack tip goes down, and middle of the crack contour x = 0 goes up.

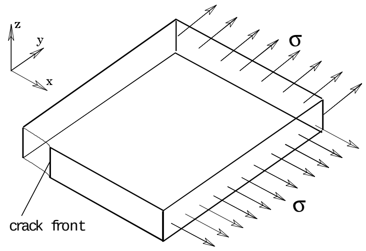

Fig. 19.

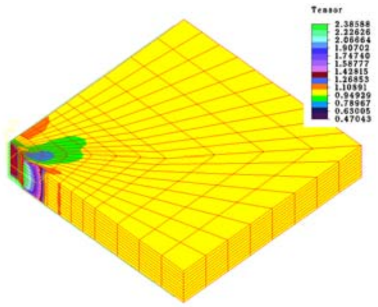

σ_x

Fig. 20.

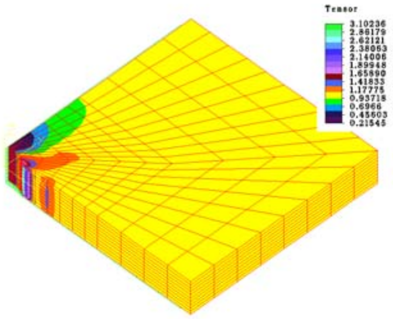

σ_y

Fig. 21.

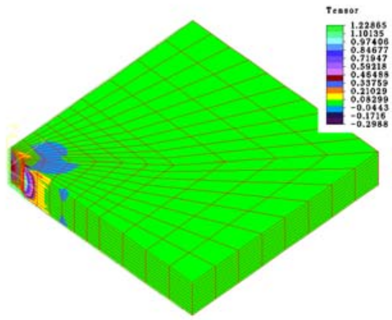

σ_z

Fig. 22.

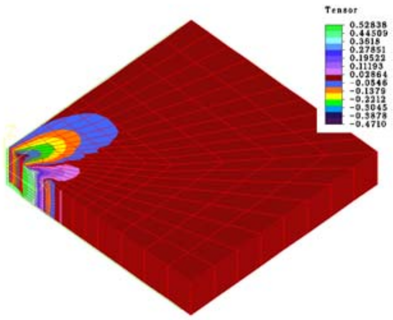

τ_{xy}

Fig. 23.

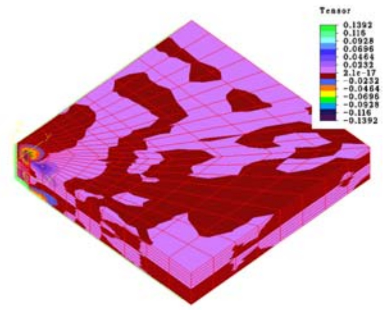

τ_{zx}

Fig. 24.

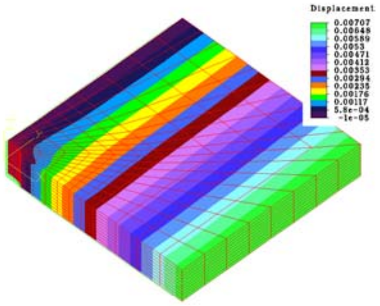

u_x

Fig. 25.

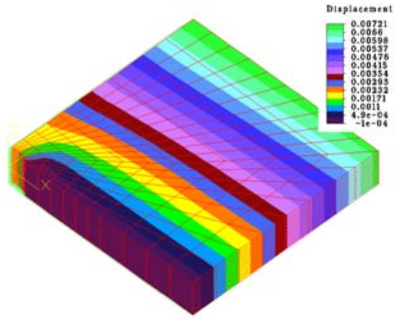

u_y

Fig. 26.

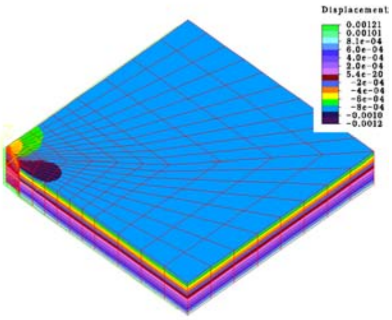

u_z

Fig. 27.

Using Kolosov-Muskhelishivili formulas [9], [14] and conformal mapping method can solve previously presented problems. The stress functions for an infinite plate under biaxial loads is [2]:

$$Z = \frac{\sigma \cdot z}{\sqrt{z^2 - a^2}}$$

where: $z = x + iy$.

Then the stresses can be determined by using relations [14]:

$$\begin{aligned} \sigma_x &= \operatorname{Re} Z - y I_m Z', \\ \sigma_y &= \operatorname{Re} Z + y I_m Z', \\ \tau_{xy} &= - y \operatorname{Re} Z'. \end{aligned} \tag{2}$$

Solutions for stress components, based on complex function and conformal mapping for elliptical contours and elliptical-hyperbolic coordinate system are given in the paper [3], [4], [5], and [6]:

$$\begin{aligned} \sigma_\rho(\rho,\varphi) = \sigma_h = & \frac{1}{gR}\Big\{\sum_{-\infty}^{\infty}\rho^{2k}\Big\{\cos 2k\varphi\,\Big(A_{2k}\Big[1-\frac{2k}{g}-\frac{6m^2}{\rho^4 g^2}\Big(1+\frac{m^2}{\rho^4}\Big)\Big]+\frac{1}{gR}B_{2k}\frac{m}{\rho^2}\Big[1+\frac{2}{(2k+1)g}\Big(1+2\frac{m^2}{\rho^4}\Big)\Big]\Big\}+ \\ & +\cos 2(k-1)\varphi\Big\{A_{2k}\Big[\frac{2km}{g\rho^2}+\frac{2m}{g^2\rho^2}\Big(1+3\frac{m^2}{\rho^4}\Big)\Big]-\frac{1}{gR}B_{2k}\frac{2m^2}{\rho^4 g(2k+1)}\Big\}+\cos 2(k-2)\varphi\Big[A_{2k}\Big(-2\frac{m^2}{\rho^4 g^2}\Big)\Big]+ \\ & +\cos 2(k+1)\varphi\Big\{A_{2k}\Big[-\frac{m}{\rho^2}-\frac{2km^3}{g\rho^6}+\frac{2m^3}{g^2\rho^6}\Big(3+\frac{m^2}{\rho^4}\Big)\Big]+\frac{1}{gR}B_{2k}\Big[-\Big(1+\frac{m^2}{\rho^4}\Big)-\frac{2m^2}{\rho^4 g(2k+1)}\Big(2+\frac{m^2}{\rho^4}\Big)\Big]\Big\}+ \\ & +\cos 2(k+2)\varphi\Big\{A_{2k}\Big[-\frac{m^2}{\rho^4}-\frac{2m^4}{g^2\rho^6}\Big]+\frac{1}{gR}B_{2k}\Big[\frac{m}{\rho^2}+\frac{2m^3}{\rho^6 g(2k+1)}\Big]\Big\}\ \Big)\ \Big\} \end{aligned} \tag{3}$$

$$
\begin{aligned}
\sigma_\varphi(\rho,\varphi)=\sigma_e=&\frac{1}{gR}\sum_{-\infty}^{\infty}A_{2k}\rho^{2k}\Big\{\ \frac{2k}{g}\Big[\ \cos 2k\varphi-\frac{m}{\rho^2}\cos 2(k-1)\varphi+\frac{m^3}{\rho^6}\cos 2(k+1)\varphi-\frac{m^2}{\rho^4}\cos 2(k+2)\varphi\ \Big]-\\
&-\frac{2m}{g^2\rho^2}\Big[\left(1+3\frac{m^2}{\rho^4}\right)\cos 2(k-1)\varphi-\frac{m}{\rho^2}\cos 2(k-2)\varphi-3\frac{m}{\rho^2}\left(1+\frac{m^2}{\rho^4}\right)\cos 2k\varphi+\frac{m^2}{\rho^4}\left(3+\frac{m^2}{\rho^4}\right)\cos 2(k+1)\varphi-\\
&-\frac{m^3}{\rho^6}\cos 2(k+2)\varphi\ \Big\}\ \Big]+\frac{1}{g^2R^2}\sum_{-\infty}^{\infty}B_{2k}\rho^{2k}\Big\{\left[\frac{m}{\rho^2}\cos 2k\varphi+\frac{m}{\rho^2}\cos 2(k+2)\varphi-\left(1+\frac{m^2}{\rho^4}\right)\cos 2(k+1)\varphi\right]+\\
&+\frac{2m}{\rho^2 g(2k+1)}\Big[\left(1+2\frac{m^2}{\rho^4}\right)\cos 2k\varphi-\frac{m}{\rho^2}\cos 2(k-1)\varphi-\frac{m}{\rho^2}\left(2+\frac{m^2}{\rho^4}\right)\cos 2(k+1)\varphi+\frac{m}{\rho^4}\cos 2(k+2)\varphi\ \Big]\ \Big\}
\end{aligned}
\tag{4}
$$

$$
\begin{aligned}
\tau_{\rho\varphi}(\rho,\varphi)=\tau_{he}=&\frac{1}{gR}\Big\{\ \sum_{-\infty}^{\infty}A_{2k}\rho^{2k}\Big\{\ \frac{2k}{g}\Big[\ \sin 2k\varphi-\frac{m}{\rho^2}\sin 2(k-1)\varphi-\frac{m}{\rho^2}\sin 2(k-1)\varphi+\frac{m^3}{\rho^6}\sin 2(k+1)\varphi-\\
&-\frac{m^2}{\rho^4}\sin 2(k+2)\varphi\ \Big]+\frac{2m}{g^2\rho^2}\Big[\ \frac{m}{\rho^2}\sin 2(k-2)\varphi-\left(1+3\frac{m^2}{\rho^4}\right)\sin 2(k-1)\varphi+3\frac{m}{\rho^2}\left(1+\frac{m^2}{\rho^4}\right)\sin 2k\varphi-\\
&-\frac{m^2}{\rho^4}\left(3+\frac{m^2}{\rho^4}\right)\sin 2(k+1)\varphi+\frac{m^3}{\rho^6}\sin 2(k+2)\varphi\ \Big]\ \Big\}\ \Big\}+\frac{1}{g^2R^2}\Big\{\ \sum_{-\infty}^{\infty}B_{2k}\rho^{2k}\Big\{\ \Big[\ \left(1+\frac{m^2}{\rho^4}\right)\sin 2(k+1)\varphi-\\
&-\frac{m}{\rho^2}\sin 2k\varphi-\frac{m}{\rho^2}\sin 2(k+2)\varphi\ \Big]+\frac{2m}{\rho^2 g(2k+1)}\Big[\ \frac{m}{\rho^2}\sin 2(k-1)\varphi-\\
&-\left(1+2\frac{m^2}{\rho^4}\right)\sin 2k\varphi+\frac{m}{\rho^2}\left(2+\frac{m^2}{\rho^4}\right)\sin 2(k+1)\varphi-\frac{m^2}{\rho^4}\sin 2(k+2)\varphi\ \Big]\ \Big\}\ \Big\}
\end{aligned}
\tag{5}
$$

Previously mentioned analytical solutions are disregarding known reality that stress state is three-dimensional at the crack tip vicinity. According to that matter of fact, known stress intensity factors determined by using two-dimensional solutions should be corrected [1], [2], [11], [12], [14], [15].

3.THREE-DIMENSIONAL STRESS AND STRAIN STATE AT THE VICINITY OF THE CRACK TIP

It is evidently from presented figures, that in all three loading cases, for plane global stress state, three-dimensional stress state is local ruling in the region close to crack tip. Strain state is undisturbed except at region of the crack. It is observed that front and back surface off the plate is not flat at the vicinity of the crack, or in other words contour line of elliptical crack does not lie in plane, and contour line is three-dimensional.

4. CONCLUSION AND DISCUSSION

For previously assumed plane global (general) stress state three-dimensional stress state at the vicinity of crack tip is obtained. It is known in literature that local stress state at crack tip region is three-dimensional, and that question is discussed in some papers [10], [13].

Knowledge of the fact that stress state is locally three-dimensional gives to us reason to develop more accurate analytical solutions and more reliable experimental methods for determining of stress and strain state at the neighbourhood of the crack [6], [7], [8].

REFERENCES

1. Gdoutos E. E., *Fracture Mechanics,* Kluwer Academic Publishers, Dordrecht, 1993
2. Broek David, *Elementary Engineering Fracture Mechanics,* Martinus Nijhoff Publishers, The Hague, 1982
3. Hedrih K., Jovanović D., (1990), *Primena funkcije kompleksne promenljive i konformnof preslikavanja za određivanje eliptično-hiperboličkih koordinata tenzora napona ravno napregnutih ploča*, XIX Jugoslovenski kongres teorijske i primenjene mehanike, Zbornik radova, pp 13-18, Ohrid
4. Hedrih K., Jovanović D., *The stress state of the elliptical-annular plate by the complex variable function and conformal mapping method*, 15 str., 73-87, časopis, Teorijska i primenjena mehanika, br. 17, Jugoslovensko društvo za mehaniku, Beograd, 1991.
5. Hedrih K., Jovanović D., *The strain state of the elliptical - annular plate by the complex variable function and conformal mapping method,* 17 str., 29-45, časopis, Teorijska i primenjena mehanika, br. 21, Jugoslovensko društvo za mehaniku, Beograd, 1995.
6. Hedrih K., Jovanović D., *Stress state around elliptical cracks in elastic plates*, International minisymposium MF Recent Advances in Fracture and Damage Mechanics, Zbornik radova, Str. 153-157, YUCTAM Vrnjačka Banja, 1997
7. Hedrih K., Jovanović D., *Fenomeni nelinearne dinamike, saznanja mehanike loma i teorije slučajnih oscilacija i projektovanje mašinskih sistema sa sigurnošću od rizika i loma*, 26. JUPITER KONFERENCIJA sa međunarodnim učešćem, Zbornik radova, Str. 3.57-3.65, Beograd, februar, 2000
8. Jovanović D., (1990), *Primena metode fotoelastičnosti za ispitivanje naponskog stanja eliptično-prstenaste ploče opterećene koncentrisanim silama*, XIX Jugoslovenski kongres teorijske i primenjene mehanike, Zbornik radova, Ohrid
9. Mushelishvili N.I., (1953), *Some Basic problems of the Mathematical Theory of Elasticity*, P. Noordhof LTD., Groningen - Holland.
10. Parsons I. D., Hall J. F., Rosakis A. J., *A Finite Element Investigation of the Elastostatic State Near a Three Dimensional Edge Crack,* SM Report 86-29, Division of Engineering and Applied Science, California Institute of Technology, Pasadena, California, 1986
11. Sedmak S. *Uvod u mehaniku loma i konstruisanje sasigurnošću od loma,* monografija, Smederevska Palanka, 1980
12. Sih G. C., *Mechanics of Fracture Initiation and Propagation,* Kluwer Academic Publishers, Dordrecht, 1990
13. Sih G. C., Lee Y. D., *Review of Triaxial Crack Border Stress and Energym Behavior,* Theroretical and Applied Fracture Mechanics, No. 12, pp. 1-17, Elsevier Science Publishers, B. V., 1989
14. Sneddon, I. N., Lowengrub, M., *Crack Problems in the Classical Theory of Elasticity* John Wiley & Sons, Inc. , New York, 1969
15. Šumarac D., Krajčinović D., *Osnovi mehanike loma,* Naučna knjiga, Graževinski fakultet, Beograd, 1990
16. Timoshenko S. P. and Goodier J. N., (1951), *Theory of Elasticity* , New York

LOKALNO STANJE NAPONA I STANJE DEFORMACIJA U OBLASTI PRSLINE ZA RAZLIČITA GLOBALNA STANJA NAPONA U PLOČI

Dragan B. Jovanović, Milena B. Jovanović

U ploči u kojoj vladaju različiti slučajevi globalnog ili opšteg stanja napona, javiće se u okolini prsline različita lokalna stanja napona i deformacija, koja su posledica međusobnog uticaja geometrije prsline i globalnog stanja napona. Uzimajući u razmatranje prslinu eliptičnog oblika (Griffith-ovu prslinu), koja se može svesti na zasek zadavanjem jedne polu-ose jednake nuli i uvodeći različita opšta naponska stanja, dobijeni su odgovarajući lokalni rasporedi napona i pomeranja u okolini takve prsline. Pošlo se od pretpostavke da je globalno stanje napona ravno, a dobijeno je trodimenzionalno stanje napona i pomeranja u okoloni prsline. Primenjena je metoda konačnih elemenata i načinjen je trodimenzionalni model ploče sa prslinom. Globalna opterećenja

su zadata tako da su naponi u delu ploče bez poremećaja usled uticaja prsline jediničnih vrednosti i izvršena je normalizacija lokalnih napona u odnosu na globalne napone.

Konvencionalna teorija ploča pretpostavlja da je unapred poznata promena napona u funkciji od koordinate z u pravcu debljine ploče. Za ravno stanje napona pretpostavlja se da je komponentni normalni napon σ_z *jednak nuli svuda u ploči, a da su naponi u ravni ploče* σ_x, σ_y *i* τ_{xy} *nezavisni od koordinate z. Ovakve pretpostavke se mogu prihvatiti pod vrlo ograničenim uslovima.*

Razmatrani su slučajevi globalnog stanja napona kada aksijalne zatežuće sile deluju u pravcu upravnom na ravan prsline ili u pravcu prsline. U radu su dati grafički prikazi rasporeda napona σ_x, σ_y, σ_z, τ_{xy}, τ_{yz}, τ_{zx}, *kao i pomeranja* u_x, u_z *i* u_z. *Pokazalo se da su komponente tenzora napona u funkciji od koordinate z u pravcu debljine ploče i da je* σ_z *različito od nule do određenog rastojanja od vrha prsline. Na osnovu dobijenih dijagrama rasporeda napona i pomeranja, doneti su zaključci o uticaju globalnog stanja napona na lokalni raspored napona i pomeranja u okolini prsline.*